Transverse Shear Deformation in Orthotropic Cylindrical Pressure Vessels Using a Higher-Order Shear Theory

S. T. Dennis* and A. N. Palazotto†
Air Force Institute of Technology, Wright-Patterson Air Force Base, Ohio

A geometrically nonlinear static shell theory allowing large displacements and rotations and parabolic transverse shear is developed. With the aid of the symbolic manipulator code MACSYMA, the theory is cast into a total Lagrangian finite-element formulation for approximate solutions. Before any nonlinear problems are undertaken, accurate linear solutions must be confirmed. The following presents several linear plate and cylindrical shell solutions, and, in particular, the effect of transverse shear deformation with increasing thickness on both isotropic and orthotropic cylindrical pressure vessels is studied. The greater the ratio of the effective laminate stiffnesses in the longitudinal vs circumferential directions of the cylindrical shell, the greater the transverse shear deformation. For the case of equal stiffness in both directions of the pressure vessel, a quasi-isotropic laminate experiences greater transverse shear deformation than does an isotropic construction.

Introduction

THE importance of transverse shear deformation in the bending behavior of thick isotropic and laminated structural elements is well documented.[1] For thicker plates and shells, classical theories can be grossly in error in predicting transverse deflections, buckling loads, or natural frequencies. Consequently, over the years, investigators have included this important effect in the analysis of these structures.[1-10] Initially, theories based on the so called Reissner-Mindlin hypothesis, which give a constant tranverse shear rotation through the thickness, were applied to flat plates[1-3] and shells.[4-7] The plate studies have shown that, as the plate became thicker, the transverse displacement normalized by the classical solution became very large, especially in laminated plates.[13] Recently, Reddy[1] has proposed a third-order shear theory characterized by parabolic transverse shear-stress distributions that gives more accurate results over the Reissner-Mindlin hypothesis when compared to elasticity solutions.[8] In addition, this theory does not requires shear correction factors nor do finite-element solutions, using cubic shape functions, evidently shear lock,[9] both drawbacks to the former theories. Reddy has solved several shell problems using the higher-order theory as well.[10]

In this paper, a geometrically nonlinear theory, which includes the parabolic transverse shear distribution through the thickness, is first developed. The theory is next cast into a total Lagrangian finite-element formulation, resulting in 28- and 36-degree-of-freedom curved rectangular elements. Linear solutions to both a flat laminated plate and then to an isotropic and laminated cylindrical presure vessel are presented. The pressure-vessel solutions are compared to a classical Love solution while letting the thickness become large, thus illustrating the effect of transverse shear deformation.

Theoretical Approach

Consider a shell geometry that can be described by orthogonal curvilinear middle-surface coordinates, ξ_1 and ξ_2, surface normal ζ, and radii of curvature, R_1 and R_2, as shown in Fig. 1. A geometrically nonlinear theory governing the shell is based on the following assumptions:

1) The shell is thin and, therefore, it is in an approximate state of plane stress, i.e., the transverse normal stress, $\sigma_3 \cong 0$. This assumption effectively reduces the generally three-dimensional behavior of the shell so that it can be described by the behavior of only a datum suface, e.g., the middle surface $\zeta = 0$.

2) The shell is restricted to small strains and consists of linear elastic laminated orthotropic material.

3) The middle surface of the shell can undergo large displacements and rotations. All nonlinear displacement terms of Green's strain displacement relations are retained for the in-plane strains, but only the linear displacement terms are retained for the transverse strains. In this way, the nonlinear displacement terms are viewed as higher order only for the transverse shear deformations. This is consistent with the thin-shell assumption of item 1.

4) The transverse shear-stress distribution is parabolic and vanishes on the top and bottom surfaces of the shell.

5) The transverse fibers of the shell are approximately inextensible so that the transverse normal strain $\epsilon_3 \cong 0$.

Constitutive Relations

From assumption 2, we consider layers of material characterized by unidirectional fibers embedded in a matrix. Each

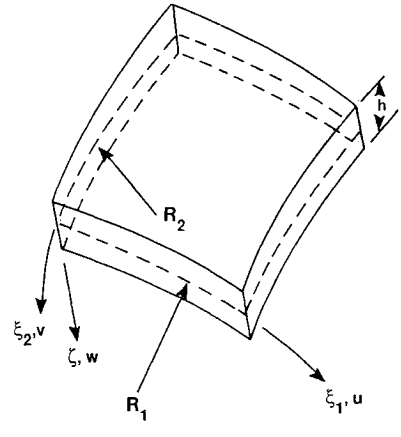

Fig. 1 Shell geometry described by orthogonal coordinates ξ_1, ξ_2, and ζ.

Received March 21, 1988; Presented as Paper 88-291 at the AIAA/ASME/ASCE AHS 29th Structures, Structural Dynamics and Materials Conference, Williamsburg, VA, April 18-20, 1988; revision received Oct. 20, 1988.

*Currently, Assistant Professor, Engineering Mechanics, U.S. Air Force Academy, CO.

†Professor, Aeronautics and Astronautics. Assistant Fellow AIAA.

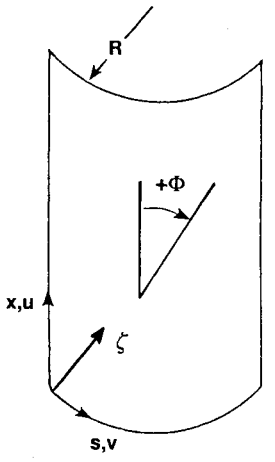

Fig. 2 Cylindrical shell with coordinates $\xi_1 = x$, $\xi_2 = s$, and ζ and ply orientation angle, Φ.

layer can be considered transversely isotropic with respect to planes perpendicular to the fiber direction. The constitutive relations in material axes for this case are as follows:

$$\begin{Bmatrix}\sigma_1\\ \sigma_2\\ \sigma_3\\ \sigma_4\\ \sigma_5\\ \sigma_6\end{Bmatrix} = \begin{bmatrix} c_{11} & c_{12} & c_{13} & 0 & 0 & 0\\ c_{12} & c_{22} & c_{23} & 0 & 0 & 0\\ c_{13} & c_{23} & c_{33} & 0 & 0 & 0\\ 0 & 0 & 0 & c_{44} & 0 & 0\\ 0 & 0 & 0 & 0 & c_{55} & 0\\ 0 & 0 & 0 & 0 & 0 & c_{66}\end{bmatrix} \begin{Bmatrix}\epsilon_1\\ \epsilon_2\\ \epsilon_3\\ \epsilon_4\\ \epsilon_5\\ \epsilon_6\end{Bmatrix} \tag{1}$$

where contracted notation is introduced, i.e., elements of the second Piola-Kirchoff stress tensor are $\sigma_i = \sigma_{ii}$ (no sum), $\sigma_4 = \sigma_{23}$, $\sigma_5 = \sigma_{13}$, $\sigma_6 = \sigma_{12}$, and similarity for the elements of Green's strain tensor, $\epsilon_i = \epsilon_{ii}$, $\epsilon_4 = 2\epsilon_{23}$, $\epsilon_5 = 2\epsilon_{13}$, and $\epsilon_6 = 2\epsilon_{12}$.

Using $\sigma_3 \cong 0$ of assumption 1 in Eq. (1) gives ϵ_3 in terms of ϵ_1 and ϵ_2. By eliminating ϵ_3 through substitution and assuming transverse isotropy, i.e., $E_2 = E_3$ and $\nu_{12} = \nu_{13}$ for fibers aligned with the 1 material axis, the constitutive relations in material axes become

$$\begin{Bmatrix}\sigma_1\\ \sigma_2\\ \sigma_3\\ \sigma_4\\ \sigma_5\end{Bmatrix} = \begin{bmatrix} Q_{11} & Q_{12} & 0 & 0 & 0\\ Q_{12} & Q_{22} & 0 & 0 & 0\\ 0 & 0 & Q_{66} & 0 & 0\\ 0 & 0 & 0 & Q_{44} & 0\\ 0 & 0 & 0 & 0 & Q_{55}\end{bmatrix} \begin{Bmatrix}\epsilon_1\\ \epsilon_2\\ \epsilon_3\\ \epsilon_4\\ \epsilon_5\end{Bmatrix} \tag{2}$$

where $Q_{ij} = C_ij - [(C_{i3}C_{j3})/C_{33}]$, in which C_{ij} are functions of engineering constants, μ_{ij}, E_i, and G_{ij}, and $C_{22} = C_{33}$, $C_{12} = C_{13}$.

For transverse isotropy, it is easily shown that

$$Q_{11} = E_1/\Delta, \quad Q_{12} = \nu_{21}/E_2/\Delta, \quad Q_{22} = E_2/\Delta$$
$$Q_{66} = G_{12}, \quad Q_{44} = G_{23}, \quad Q_{55} = G_{13} \tag{3}$$

where $\Delta = 1 - \nu_{12}\nu_{12}$.

Now consider a shell that is constructed of layers of the material described earlier. In general, the fibers of the kth inidividual layer of ply are oriented at an angle Φ, as shown in Fig. 2 for a cylindrical shell with coordinates $\xi_1 = x$, $\xi_2 = s$, and ξ. Therefore, the constitutive relations of Eq. (2) for that ply must be transformed into shell coordinates resulting in Eqs. (4).

$$\begin{Bmatrix}\sigma_1\\ \sigma_2\\ \sigma_6\end{Bmatrix}^k = \begin{bmatrix}\bar{Q}_{11} & \bar{Q}_{12} & \bar{Q}_{16}\\ & \bar{Q}_{22} & \bar{Q}_{26}\\ & & \bar{Q}_{66}\end{bmatrix}^k \begin{Bmatrix}\epsilon_1\\ \epsilon_2\\ \epsilon_6\end{Bmatrix} \tag{4a}$$

$$\begin{Bmatrix}\sigma_4\\ \sigma_5\end{Bmatrix}^k = \begin{bmatrix}\bar{Q}_{44} & \bar{Q}_{45}\\ & \bar{Q}_{55}\end{bmatrix}^k \begin{Bmatrix}\epsilon_4\\ \epsilon_5\end{Bmatrix} \tag{4b}$$

where $\bar{Q}_{ij}$ $(i,j = 1,2,6)$ and $\bar{Q}_{mn}$ $(m,n = 4,5)$ are elements of symmetric arrays of transformed stiffness for the kth ply, and σ_k and ϵ_k are measured with respect to shell coordinates ξ_α $(\alpha = 1,2)$ and ξ $(= 1)$.

Therefore, from Eq. (2) or (4), if the transverse stresses α_4 and σ_5 vanish on the top and bottom surfaces of the shell, as stated in assumption 4, it is also true that the transverse shear strains vanish on those surfaces.

Kinematics

Let the following truncated power series in the transverse coordinate ζ represent the continuum displacements of the shell.

$$u_1(\xi_1,\xi_2,\zeta) = u(1 - \zeta/R_1) + \zeta\psi_1 + \zeta^2\phi_1 + \zeta^3\gamma_1 + \zeta^2\phi_1 \tag{5a}$$

$$u_2(\xi_1,\xi_2,\zeta) = v(1 - \zeta/R_2) + \zeta\psi_2 + \zeta^2\phi_2 + \zeta^3\gamma_2 + \zeta^4\theta_2 \tag{5b}$$

$$u_3(\xi_1,\xi_2) = w \tag{5c}$$

where u, v, w, ψ_α, ϕ_α, γ_α, and θ_α are functions of ξ_α, and ψ_α are bending rotations of the normals. The functions ϕ, γ, and θ are determined such that the transverse shear stress vanishes on the top and bottom surfaces of the shell.

In Eqs. (5), the transverse displacement u_3 is not a function of ζ. This will give $\epsilon_3 = 0$ when only linear displacement terms retained from the strain displacement relations. However, as shown, ϵ_3 is included via the constitutive relations of Eqs. (2) and (4).

The assumed displacements of Eqs. are slightly more involved than those assumed in the literature for flat plates.[1] For a plate, only third-order terms in the transverse coordinate ζ are necessary to give the desired parabolic transverse shear-stress distributions. However, shell structures, due to their curved surfaces, have coupling between displacements that plates do not possess and the fourth-order terms become necessary. Ultimately, the kinematics will closely resemble the plate kinematics in Ref. 1. In addition, Reddy[10] arrives at identical general shell kinematics as derived here but uses a different approach.

Keeping only the linear displacement terms from Green's strain displacement relations, the transverse shear strains become

$$\epsilon_4 = (1/h_2)(u_{3,2} + h_2u_{2,3} - u_2h_{2,3}) \tag{6a}$$

$$\epsilon_5 = (1/h_1)(u_{3,1} + h_1u_{1,3} - u_1h_{1,3}) \tag{6b}$$

where $(),_\alpha$ refers to differentiation with respect to ξ_α; $(),_3$ refers to differentiation with respect to ζ; and the shell scale factors $h_\gamma = \alpha_\gamma(1 - \zeta/R_\gamma)$ (no sum on γ, $\gamma = 1,2$) and α_γ are square roots of elements of the surface metric.

Using Eqs. (5) in Eq. (6a) and assuming zero transverse shear stress and, therefore, strain, on the shell boundaries, one obtains

$$\phi_2 = 0 \tag{7a}$$

$$\theta_2 = \gamma_2/2R_2 \tag{7b}$$

$$[1 - (h^2/\underline{8R_2^2}]\,\gamma_2 \approx \gamma_2 = (-4/3h^2)[\psi_2 + (w,_2/\alpha_2)] \tag{7c}$$

Assume, for the moment, that we have a fairly thick shell, i.e., let $R_2 = 5h$. In this case, the underlined term in Eq. (7c) is still only 0.005 and, therefore, can be neglected compared to 1 as indicated. Futhermore, we can neglect the fourth-order term of Eqs. (5b) and (7) since it is only one-twentieth of the third-order term. A similar exercise is applied to θ_5. Equations (7) and Eqs. (5) then give the following for the general shell kinematics:

$$u_1(\xi_1,\xi_2,\zeta) = u(1 - \zeta/R_1) + \zeta\psi_1 + \zeta^3 k[\psi_1 + (w,_1/\alpha_1)] \quad (8a)$$

$$u_2(\xi_1,\xi_2,\zeta) = v(1 - \zeta/R_2) + \zeta\psi_2 + \zeta^3 k[\psi_2 + w,_2/\alpha_2)] \quad (8b)$$

$$u_3(\xi_1,\xi_2) = w \quad (8c)$$

where $k = -4/3h^2$.

Strain Displacement Relations

Next, the strains are found via the Green's strain displacement relations where, again, all nonlinear displacement terms are retained for the in-plane strains, but only linear displacement terms are retained for the transverse strains. After scale-factor expressions are approximated by truncated binomial series, the in-plane strains can be represented as in Eq. (9), where the terms extend to ζ^7. the ϵ_i^0 and κ_{ip} terms represent algebraically complicated nonlinear terms in displacement and are functions of the surface parameters ζ_1 and ζ_2. On the other hand, the transverse strains are linear and are written simply in Eqs. (10). Each of the strain components, ϵ_i^0 and κ_{ip} of Eq. (9), as well as ϵ_4 and ϵ_5 of Eqs. (10), are specialized for the cylindrical coordinates x and s of Fig. 2 and are shown in the Appendix.

$$\epsilon_i = \epsilon_i^0 + \zeta^p \kappa_{ip}, \qquad i = 1,2,6,\ p = \text{sum 1 to 7} \quad (9)$$

$$\epsilon_4 = [(w,_2/\alpha_2) + \psi_2](1 + 3k\zeta^2) \quad (10a)$$

$$\epsilon_5 = [(w,_1/\alpha_1) + \psi_1](1 + 3k\zeta^2) \quad (10b)$$

Potential Energy

The total potential energy of the shell, Π_p, is given by Eq. (11), where U_1 and U_2 are the internal strain energy expressions corresponding to the in-plane and transverse terms, respectively, and V represents the work done by external forces.

$$\Pi_p = U_1 + U_2 + V \quad (11)$$

Equation (11) is more easily manipulated if the following quantities are defined. First, rewrite Eq. (9) as shown in Eq. (12). Then, the in-plane strain energy can be rewritten using Eq. (2) as developed in Eq. (13).

$$\mathcal{E} = \mathcal{E}^0 + \mathcal{K}\mathcal{Z} \quad (12)$$

where

$$\mathcal{E} = \begin{Bmatrix} \epsilon_1 \\ \epsilon_2 \\ \epsilon_6 \end{Bmatrix}, \qquad \mathcal{E}^0 = \begin{Bmatrix} \epsilon_1^0 \\ \epsilon_2^0 \\ \epsilon_6^0 \end{Bmatrix}, \qquad \mathcal{Z} = \begin{Bmatrix} \zeta \\ \zeta^2 \\ \cdot \\ \cdot \\ \cdot \\ \zeta^7 \end{Bmatrix}$$

$$\mathcal{K} = \begin{bmatrix} \kappa_{11} & \kappa_{12} & \cdots & \kappa_{17} \\ \kappa_{21} & \kappa_{22} & \cdots & \kappa_{27} \\ \kappa_{61} & \kappa_{62} & \cdots & \kappa_{67} \end{bmatrix}$$

and let

$$\mathcal{Q} = \begin{bmatrix} \bar{Q}_{11} & \bar{Q}_{12} & \bar{Q}_{16} \\ & \bar{Q}_{22} & \bar{Q}_{26} \\ & & \bar{Q}_{66} \end{bmatrix}^k$$

$$U_1 = \frac{1}{2}\int_\Omega \int_h (\mathcal{Q}\mathcal{E})^T \mathcal{E}\, d\zeta d\Omega$$

$$= \frac{1}{2}\int_\Omega \int_h \{\mathcal{E}^{0T}\mathcal{Q}\mathcal{E}^0 + 2\mathcal{E}^{0T}\mathcal{Q}\mathcal{K}\mathcal{Z} + \mathcal{Z}^T(\mathcal{K}^T\mathcal{Q}\mathcal{K})\mathcal{Z}\, d\zeta\}\, d\Omega$$

$$= \frac{1}{2}\int_\Omega \int_h \{\epsilon_j^0 \epsilon_i^0 \bar{Q}_{ij} + 2\epsilon_j^0 \bar{Q}_{ij}\kappa_{ip}\zeta^p + \kappa_{jp}\kappa_{ir}\bar{Q}_{ij}\zeta^{p+r}\, d\zeta\}\, d\Omega \quad (13)$$

where $i,j = 1,2,6$ and $p,r =$ sum 1 to 7, $\Omega =$ shell midplane. The last expression of Eq. (13) hints at the complexity of the in-plane strain energy of the shell. The energy is comprised of a multitude of squares of the strain components, ϵ_i^0 and κ_{ip}, due to summations on four different indices. Furthermore, each ϵ_i^0 and κ_{ip} consists of many displacement terms, see the Appendix for cylindrical shell specilization.

Finally, the result of Eq. (13) is written concisely in terms of an area integral representing the shell midsurface in Eq. (14), where the ζ dependence has been integrated by defining a series of elasticity arrays shown in Eq. (15). The u_k of Eq. (14) are written in terms of strain components and these elasticity arrays in the Appendix. For linear analyses, the arrays L, P, R, S, and T are not used. In addition, for symmetrically arranged laminates, the elements of the elasticity arrays associated with odd powers of ζ are identically zero.

$$u_1 = \frac{1}{2}\int_\Omega (u_1 + u_2 + u_3)\, d\Omega \quad (14)$$

$$[A_{ij}, B_{ij}, D_{ij}, E_{ij}, F_{ij}, G_{ij}, H_{ij}, I_{ij}, J_{ij}, K_{ij}, L_{ij},$$

$$P_{ij}, R_{ij}, S_{ij}, T_{ij}] = \int_h \bar{Q}_{ij}\,[1,\zeta,\zeta^2,\zeta^3,\zeta^4,\zeta^5,\zeta^6,\zeta^7,$$

$$\zeta^8,\zeta^9,\zeta^{10},\zeta^{11},\zeta^{12},\zeta^{13},\zeta^{14}]\, d\zeta \quad (15)$$

where $i,j = 1,2,6$.

A similar manipulation is performed on the transverse shear energy U_2 as shown in Eq. (16), where shear elasticity arrays have also been defined.

$$U_2 = \frac{1}{2}\int_\Omega (\epsilon_m^0 \epsilon_m^0 A_{mn} + 2\epsilon_n^0 \kappa_{m2} D_{mn} + \kappa_{n2}\kappa_{m2} F_{mn})\, d\Omega$$

$$[A_{mn}, D_{mn}, F_{mn}] = \int_h \bar{Q}_{mn}[1,\zeta^2,\zeta^4]\, d\zeta \quad (16)$$

where $m,n = 4,5$; $\epsilon_4^0 = w,_2/\alpha_2 + \psi_2$; $\epsilon_5^0 = w,_1/\alpha_1 + \psi_1$; $\kappa_{42} = 3k\epsilon_4^0$; and $\kappa_{52} = 3k\epsilon_5^0$.

Finite-Element Solution

The shell domain is discretized such that the continuum displacements are approximated by nodal values and interpolation functions. The displacement gradient vector, d, is defined based on the unique displacement terms of the strain displacement relations. Presently, for a cylindrical shell geometry, d is an 18×1 array given in Eq. (17), and EQ. (18) shows the relationship between d and the vector of nodal displacement unknowns, q.

$$d^T = \{uu,_1\ u,_2\ vv,_1\ v,_2\ ww,_1\ w,_2\ w,_{11}\ w,_{22}\ w,_{12}\ \psi_1\ \psi_{1,1}\ \psi_{1,2}$$

$$\psi_2\ \psi_{2,1}\ \psi_{2,2}\} \quad (17)$$

$$d = \mathcal{D}q \quad (18)$$

Table 1 Flat plate, aspect ratio = 3 ($\bar{w} = 100 w_c h^3 E_2/qa^4$, w_c = center deflection, h = thickness, q = pressure, a = short side length of plate. $E_1 = 37.5 \times 10^6$ psi, $E_2 = 1.5 \times 10^6$, $G_{12} = G_{13} = 0.75 \times 10^6$, $G_{23} = 0.3 \times 10^6$, $\nu_{12} = 0.25$

a/h	Theory	$\bar{w}$
4	Pagano (3-D)	2.82
	R-M	2.36
	Reddy (Navier)	2.64
	FEM	2.65
10	Pagano (3-D)	0.919
	R-M	0.803
	Reddy (Navier)	0.862
	FEM	0.864
20	Pagano (3-D)	0.610
	R-M	0.578
	Reddy (Navier)	0.594
	FEM	0.595
100	Pagano (3-D)	0.508
	R-M	0.506
	Reddy (Navier)	0.507
	FEM	0.507
	CLPT	0.503

where $\mathfrak{D}$ is an array of interpolation functions and their derivatives.

The potential energy is then given for the discretized domain in Eq. (19). The first variation of the energy, $\delta\Pi_p$, gives the equilibrium equations, also shown in Eqs. (19). The symmetric arrays K, N_1, and N_2 were defined from Eqs. (9), (10), and (14), and (16) using a generalization of the approach described by Rajasekaran and Murray.[11] As discussed earlier, the assumed nonlinearity and the parabolic transverse shear-stress distribution, together with a shell geometry, introduce an algebraic complexity not usually seen. As a consequence, arrays K, N_1, and N_2 were formed by the symbolic manipulator code MACSYMA.[12] In this way, hundreds of large-dimension array multiplications were accomplished once by a computer independent of any finite-element calculations. The resulting expressions for K, N_1, and N_2 then were programmed and included as subroutines in the finite-element coding. The aforementioned matrix multiplications cannot practically be carried out by hand without major simplifications in the strain displacement relations. In a linear analysis, we do not call the subroutines that calculate the elements of N_1 and N_2 since they are functions of displacement and are, therefore, nonlinear terms.

$$\Pi_p = (q^T/2)\int_\Omega \mathfrak{D}^T [K + (N_1/3) + (N_2/6)]\, \mathfrak{D}\, d\Omega q - q^T R \quad (19a)$$

$$\delta\Pi_p = \delta q^T \int_\Omega \mathfrak{D}^T [K + (N_1/2) + (N_2/3)]\, \mathfrak{D}\, d\Omega\, q - \delta q^T R = 0 \quad (19b)$$

where R is a column array of the nodal loads, K an array of constant stiffness coefficients, N_1 an array of stiffness coefficients that are linear in displacement, and N_2 an array of stiffness coefficients that are quadratic in displacement.

Rectangular flat and curved elements with four and eight nodes have been developed for plates and cylindrical shells, respectively. The four-noded element has 28 degrees of freedom (dof) and assumes linear distributions for the in-plane displacements u and v, and the bending rotations ψ_α. The remaining nodal dof, w, and its two first derivatives are interpolated by nonconforming cubic shape functions. The eight-noded element has the same features as the four-noded element, except u and v are quadratically interpolated resulting in 36 dof.

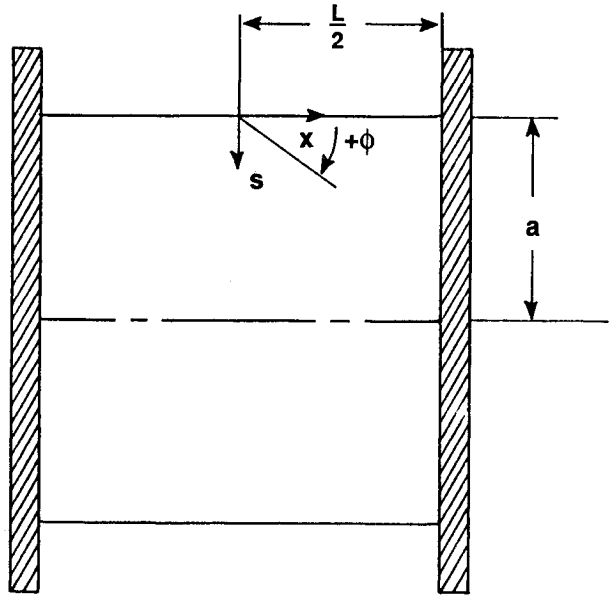

Fig. 3 Cylindrical pressure vessel, longitudinal coordinate, x; circumferential, s; radius, $a = 30$ in.; length, $L = 60$ in.; $E = 4.5 \times 10^5$ psi, $\nu = 0.3$ for isotropic. $E_1 = 2.5 \times 10^7$, $E_2 = 4.5 \times 10^5$, $\nu_{12} = 0.25$, $G_{12} = G_{13} = 0.5 \times 10^6$, $G_{23} = 0.2 \times 10^6$ for laminate.

The finite-element formulation is tested vs many known plate and shell solutions; two linear cases are presented here.

Linear Results

Laminated Plate

A [0/90/0] simply supported rectangular plate with an aspect ratio of 3 under sinusoidal transverse pressure loading serves as a linear flat-plate verification of the finite-element formulation. This problem has been solved by Pagano based on three-dimensional elasticity. Classical laminated plate theory (CLPT), Reissner-Mindlin (R-M) plate theory, and a Navier series parabolic transverse shear solutions are presented by Reddy.[1] The present theory, when reduced for a linear flat plate, is very similar to Reddy's linear parabolic transverse shear solution and, therefore, represents an excellent initial test case for the finite-element (FEM) formulation of this study. The results are tabulated in Table 1, and we can see that the finite-element solutions, using a 4×4 mesh to model one-quarter of the plate, very closely resemble Reddy's exact solution. The effects of transverse shear deformation are evident as the thickness of the plate is increased. Also, the higher-order theory is considerably more accurate than the other theories when compared to the elasticity solution.

Cylindrical Pressure Vessel

A pressure vessel with rigid end plates under pressure, p, as shown in Fig. 3, serves as a cylindrical shell verification test. An orthotropic classical solution is found in Ref. 13. Upon verification of the finite-element model, a thickness study was carried out to determine the effect of transverse shear deformation. In this study, only the thickness of the shell, h, was varied, while the length, L, and the radius, a, were kept constant. Normalized transverse displacement for three points along the x axis are shown in Fig. 4, where the classical solution is represented by $\bar{w} = 1$. As can be seen, the tranverse shear deformation begins to influence the displacement for $L/h \leq 40$ for points of the cylinder near the clamped edge. This region experiences significant bending compared to the center of the cylinder, where mostly membrane action occurs. Increased bending also gives more transverse shear deformation and, therefore, the normalized displacements, $\bar{w}$, are larger.

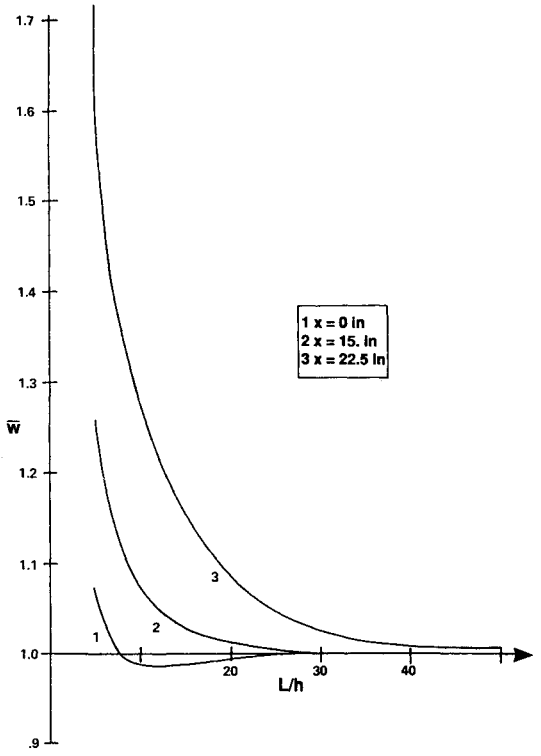

Fig. 4 Isotropic pressure vessel, normalized transverse displacement, $\bar{w}$.

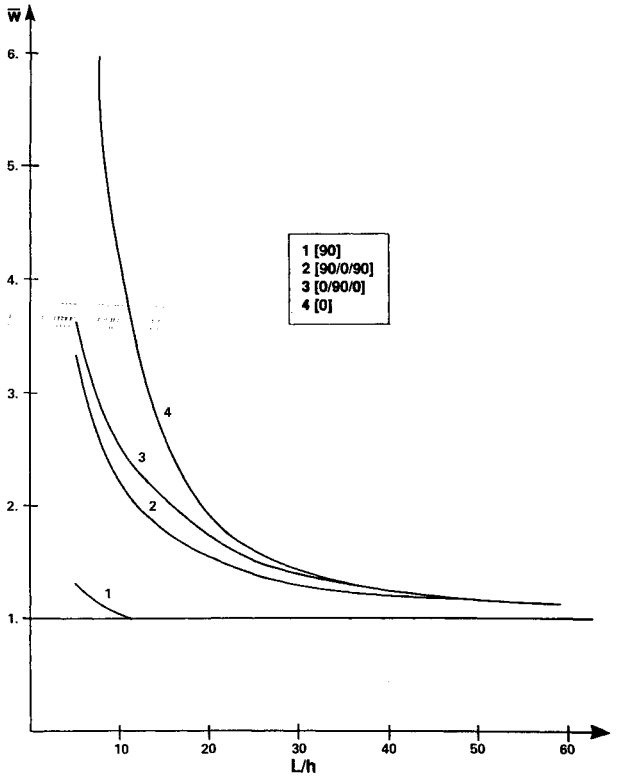

Fig. 5 Orthropic pressure vessel, normalized displacement, $\bar{w}$ (x = 22.5 in.).

A similar study was performed on laminated cylinders with ply orientations of [90/0/90], [0/90/0], and [0]. The results are plotted in Fig. 5 for $x = 22.5$ in. Effective laminate stiffness properties, E_x and E_s, were used in the classical solution for the nonunidirectional laminates, whereas $E_1 = W_x$, $E_2 = E_s$ and $E_2 = E_x$, $E_1 = E_s$ are used for the unidirectional laminates [0] and [90], respectively. The plot indicates that, for the laminates where $E_x > E_s$, more transverse shear deformation occurs. The hoop stress for these cases deviates more from a nominal membrane stress, pa/h, thus indicating more bending.

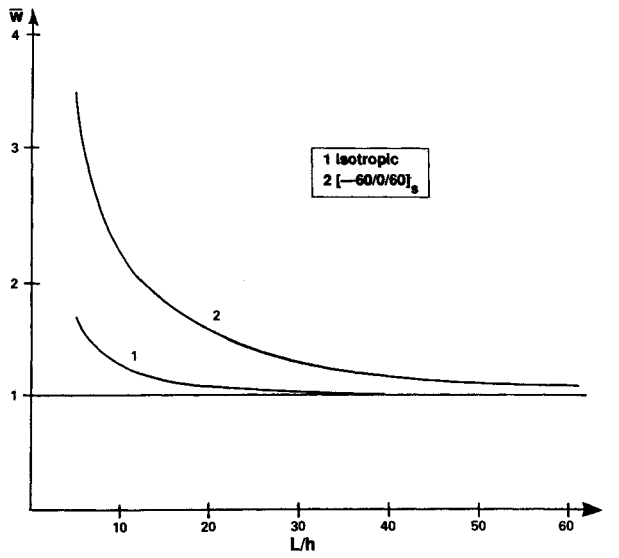

Fig. 6 Isotropic and quasi-isotropic pressure vessels, normalized displacement, $\bar{w}$ ($x = 22.5$ in.).

Lastly, the quasi-isotropic laminate $[-69/0/60]_s$ was analyzed and compared to the isotropic case. The results for $x = 22.5$ in. are shown in Fig. 6. The composite construction is influenced by the shear deformation to a greater extent than the isotropic. Since $E_x = E_s$ for both the quasi-isotropic and the isotropic constructions, we conclude that the difference is due to the orthotropy ($E_1 \neq E_2$) of the quasi-isotropic laminate.

An interesting result was noted in the isotropic cylinder at $x = 0$ (see Fig. 4) and in the laminated cylinders where $E_x < E_s$. In Fig. 4, note that the curve for $x = 0$ dips slightly below $\bar{w} = 1$ for values of L/h of approximately 10–20. For these cases, a countershear point, i.e., where the transverse shear rotation changes sign, gives transverse displacements that are less than those given by the classical solution. In contrast, the flat plate always has a shear rotation that gives a larger transverse displacement.

Conclusions

A geometrically nonlinear shell theory results in ζ^7 in the strain displacement relations and the definition of many new elasticity arrays. For linear analyses, the higher the ratio E_x/E_s in the cylindrical pressure vessels, the greater the normalized displacement, $\bar{w}$. When $E_x = E_s$, the quasi-isotropic construction is influenced by shear deformation to a greater degree than is the isotropic.

Appendix

Cylindrical Shell Strain Displacement Components, $c = 1/R$

$$\epsilon_1 = \epsilon_1^0 + \zeta^p \kappa_{1p}, \tag{A1}$$

$$\epsilon_1^0 = u_{,1} + \tfrac{1}{2}(u_{,1}^2 + v_{,1}^2 + w_{,1}^2) \tag{A2}$$

$$\kappa_{11} = \kappa_{1,1} - v_{,1}^2 c^2 + \psi_{1,1} u_{,1} + \psi_{2,1} v_{,1} \tag{A3}$$

$$\kappa_{12} = v_{,1}^2 c^2/2 - \psi_{2,1} v_{,1} c + \tfrac{1}{2}(\psi_{1,1}^2 + \psi_{2,1}^2 \tag{A4}$$

$$\kappa_{13} = k(w_{,11} + \psi_{1,1}) + u_{,1} k(w_{,11} + \psi_{1,1}) + v_{,1} k(w_{,21} + \psi_{2,1}) \tag{A5}$$

$$\kappa_{14} = -v_{,1}kc(w_{,21} + \psi_{2,1}) + \psi_{1,1}k(w_{,11} + \psi_{1,1}) + \psi_{2,1}k(w_{,21} + \psi_{2,1} \quad \text{(A6)}$$

$$\kappa_{15} = 0 \quad \text{(A7)}$$

$$\kappa_{16} = (k/2)^2(w_{,11}^2 + 2w_{,11}\psi_{1,1} + \psi_{1,1}^2 + w_{,21}^2 + 2w_{,21}\psi_{2,1} + \psi_{2,1}^2 + \psi_{2,1}^2) \quad \text{(A8)}$$

$$\kappa_{17} = 0 \quad \text{(A9)}$$

$$\epsilon_2 = \epsilon_2^0 + \zeta^p\kappa_{2p'} \quad \text{(A10)}$$

$$\epsilon_2^0 = v_{,2} - wc + \tfrac{1}{2}(v_{,2}^2 + w_{,2}^2 + u_{,2}^2 + v^2c^2 + w^2c^2) + vw_{,2}c - v_{,2}wc \quad \text{(A11)}$$

$$\kappa_{21} = \psi_{2,2} - wc^2 + u_{,2}^2c + w_{,2}^2c + w^2c^3 - c^2(v_{,2}w - vw_{,2}) + v\psi_2c^2 + v_{,2}\psi_{2,2} + u_{,2}\psi_{1,2} - c(\psi_{2,2}w - \psi_2w_{,2}) \quad \text{(A12)}$$

$$\kappa_{22} = \psi_{2,2}c + \tfrac{1}{2}(\psi_{2,2}^2 + \psi_{1,2}^2 + \psi_2^2c^2) + 2\psi_{1,2}u_{,2}c + v\psi_2c^3 + -2c^2(\psi_{2,2}w - \psi_2w_{,2}) + \psi_{2,2}v_{,2}c \quad \text{(A13)}$$

$$\kappa_{23} = k(w_{,22} + \psi_{2,2}) + c(\psi_{2,2}^2 + \psi_{1,2}^2) + ku_{,2}(w_{,12} + \psi_{1,2}) + w_{,2}kc(w_{,2} + \psi_2) + vkc^2(w_{,2} + \psi_2) - wkc(w_{,22} + \psi_{2,2}) + \psi_2^2c^3 + kv_{,2}(w_{,22} + \psi_{2,2}) \quad \text{(A14)}$$

$$\kappa_{24} = kc(w_{,22} + \psi_{2,2}) + 2u_{,2}kc(w_{,12} + \psi_{1,2}) + v_{,2}kc(w_{,22} + \psi_{2,2}) + vkc^3(w_{,2} + \psi_2) + k\psi_{2,2}(w_{,22} + \psi_{2,2} + 2kc^2(-ww_{,22} - w\psi_{2,2} + w_{,2}^2 + w_{,2}\psi_2)\psi_{1,2}k(w_{,12} + \psi_{1,2}) + \psi_2kc^2(w_{,2} + \psi_2) \quad \text{(A15)}$$

$$\kappa_{25} = 2kc[\psi_{2,2}(w_{,22} + w_{2,2}) + \psi_{1,2}(w_{,12} + \psi_{1,2}) + \psi_2c^2(w_{,2} + \psi_2)] \quad \text{(A16)}$$

$$\kappa_{26} = (k^2/2)[w_{,22}^2 + 2w_{,22}\psi_{2,2} + \psi_{2,2}^2 + w_{,12}^2 + 2w_{,12}\psi_{1,2} + \psi_{1,2}^2 + c^2(w_{,2}^2 + 2w_{,2}\psi_2 + \psi_2^2] \quad \text{(A17)}$$

$$\kappa_{27} = k^2c[(w_{,22} + \psi_{2,2})^2 + (w_{,12} + \psi_{1,2})^2 + c^2(w_{,2} + \psi_2)^2 \quad \text{(A18)}$$

$$\epsilon_6 = \epsilon_6^0 + \zeta^p\kappa_{6p'} \quad \text{(A19)}$$

$$\epsilon_6^0 = u_{,2} + v_{,1} + u_{,1}u_{,2} + v_{,1}v_{,2} + w_{,1}w_{,2} + c(vw_{,1} - v_{,1}w) \quad \text{(A20)}$$

$$\kappa_{61} = c(u_{,2} - v_{,1}) + \psi_{1,2} + \psi_{2,1} + u_{,1}\psi_{1,2} + \psi_{1,1}u_{,2}c (u_{,1}u_{,2} - v_{,1}v_{,2} + w_{,1}w_{,2} + w_{,1}w_{,2} - w\psi_{2,1} + w_{,1}\psi_2) + v_{,1}\psi_{2,2} + v_{,2}\psi_{2,1} \quad \text{(A21)}$$

$$\kappa_{62} = c(\psi_{1,2} + u_{,1}\psi_{1,2} + u_{,2}\psi_{1,1} - cw\psi_{2,1} + cw_{,1}\psi_2) + \psi_{1,1}\psi_{1,2} + \psi_{2,1}\psi_{2,2} \quad \text{(A22)}$$

$$\kappa_{63} = 1kw_{,12} + k\psi_{1,2} + k\psi_{2,1} + ku_{,2}(w_{,11} + \psi_{1,1}) + kcw_{,1}(w_{,2} + \psi_2) + ku_{,1}(w_{,12} + \psi_{1,2}) + kv_{,1}(w_{,22} + \psi_{2,2}) - kcw(w_{,12} + \psi_{2,1}) + c(\psi_{1,1}\psi_{1,2} + \psi_{2,2}) + kv_{,2}(w_{,12} + \psi_{2,1}) \quad \text{(A23)}$$

$$\kappa_{64} = kc(w_{,12} + \psi_{1,2}) + kcu_{,2}(w_{,11} + \psi_{1,1} + kcu_{,1}(w_{,12} + \psi_{1,2}) + \psi_{2,1}(w_{,22} + \psi_{2,2}) + \psi_{2,2}(w_{,12} + \psi_{2,1}) - kc^2(ww_{,12} + w_{,1}w_{,2} - w_{,1}\psi_2) + k(\psi_{1,1}w_{,12} + 2\psi_{1,1}\psi_{1,2} + \psi_{1,2}w_{,11}) \quad \text{(A24)}$$

$$\kappa_{65} = kc(\psi_{1,1}w_{,12} + \psi_{1,2}w_{,11} + \psi_{2,1}w_{,22} + \psi_{2,2}w_{,12} + 2\psi_{1,1}\psi_{1,2} + 2\psi_{2,1}\psi_{2,2}) \quad \text{(A25)}$$

$$\kappa_{66} = k^2[(w_{,11} + \psi_{1,1})(w_{,12} + \psi_{1,2}) + (w_{,12} + \psi_{2,1})(w_{,22} + \psi_{2,2})] \quad \text{(A26)}$$

$$\kappa_{67} = k^2c[(w_{,11} + \psi_{1,1})(w_{,12} + \psi_{1,2}) + (w_{,12} + \psi_{2,1})(w_{,22} + \psi_{2,2})] \quad \text{(A27)}$$

$$\epsilon_4 = (w_{,2} + \psi_2) + 3\zeta^2k(w_{,2} + \psi_2) \quad \text{(A28)}$$

$$\epsilon_5 = (w_{,1} + \psi_1) + 3\zeta^2k(w_{,1} + \psi_1) \quad \text{(A29)}$$

In-plane Internal Strain Energy Expression in Terms of Strain Components

$$U_1 = \frac{1}{2}\int_\Omega (u_1 + u_2 + u_3)\, d\Omega \quad \text{(A30)}$$

$$u_1 = \epsilon_j^0\epsilon_i^0A_{ij} \quad \text{(A31)}$$

$$u_2 = 2\epsilon_j^0(\kappa_{i1}B_{ij} + \kappa_{i2}D_{ij} + \kappa_{i3}E_{ij} + \kappa_{i4}F_{ij} + \kappa_{i5}G_{ij} + \kappa_{i6}H_{ij} + \kappa_{i7}I_{ij}) \quad \text{(A32)}$$

$$u_3 = \kappa_{j1}\kappa_{i1}D_{ij} + 2\kappa_{j1}\kappa_{i2}E_{ij} + (2\kappa_{j1}\kappa_{i3} + \kappa_{j2}\kappa_{i2})F_{ij} + 2(\kappa_{j1}\kappa_{i4} + \kappa_{j2}\kappa_{i3})G_{ij} + (2\kappa_{j1}\kappa_{i5} + 2\kappa_{j2}\kappa_{i4})H_{ij} + 2(\kappa_{j1}\kappa_{i6} + \kappa_{j2}\kappa_{i5} + \kappa_{j3}\kappa_{i4})I_{ij} + (2\kappa_{j1}\kappa_{i7} + 2\kappa_{j2}\kappa_{i6} + 2\kappa_{j3}\kappa_{i5} + \kappa_{j4}\kappa_{i4})J_{ij} + 2(\kappa_{j2}\kappa_{i7} + \kappa_{j3}\kappa_{i6} + \kappa_{j4}\kappa_{i5})K_{ij} + (2\kappa_{j3}\kappa_{i7} + 2\kappa_{j4}\kappa_{i6} + \kappa_{j5}\kappa_{i5})L_{ij} + 2(\kappa_{j4}\kappa_{i7} + \kappa_{j5}\kappa_{i6})P_{ij} + (2\kappa_{j5}\kappa_{i7} + \kappa_{j6}\kappa_{i6})R_{ij} + 2\kappa_{j6}\kappa_{i7}S_{ij} + \kappa_{j7}T_{ij} \quad \text{(A33)}$$

Acknowledgment

This work is sponsored by the Air Force Office of Scientific Research under Grant AFOSR-88-0010.

References

[1]Reddy, J. N., *Energy and Variational Methods in Applied Mechanics*, Wiley, 1984.

[2]Mindlin, R. D., "Influence of Rotatory Inertia and Shear on Flexural Motion of Isotropic Elastic Plates," *Journal of Applied Mechanics*, Vol. 18, pp. 31–38.

[3]Yang, Norris, Stavsky, "Elastic Wave Propagation in Heterogeneous Plates,' *International Journal of Solid Structures*, Vol. 2, 1966, pp. 665–684.

[4]Hildebrand, F. B., Reissner, E., and Thomas, G. B., "Notes on the Foundations of the Theory of Small Displacements of Orthotropic Shells," NACA Rept. 1833, 1949.

[5]Gulati, S. T. and Essenberg, F., "Effects on Anisotropy in Axisymmetric Cylindrical Shells," *Journal of Applied Mechanics*, Vol. 34, pp. 659–666.
[6]Zukas, J. A. and Vinson, J. R., "Laminated Shells," *Journal Engineering Mechanics*, Vol. 38, 1971, pp. 400–407.
[7]Reddy, J. N., "Exact Solutions of Moderately Thick Laminated Shells," *Journal of Engineering Mechanics*, Vol. 110, May 1984, pp. 794–809.
[8]Pagano, N. J., "Exact Solutions for Rectangular Bidirectional Composites and Sandwich Plates," *Journal of Computational Materials*, Vol. 4, pp. 20–34.
[9]Cook, R. D., *Concepts and Applications of Finite Element Analysis*, Wiley, 1981, pp. 261–262.
[10]Reddy, J. N. and Liu, C. F., "A Higher Order Shear Deformation Theory of Laminated Elastic Shells," *International Journal of Engineering Science*, Vol. 23, No. 3, 1985, pp. 319–330.
[11]Rajasekaran, S., and Murray, D. W., "Incremental Finite Element Matrices," *Journal of Structures Division*, ASCE, Dec. 1973, pp. 2423–2437.
[12]*VAX UNIX MACSYMA Reference Manual*, Symbolics, Inc., 1985.
[13]Kraus, H., *Thin Elastic Shells*, Wiley, 1967.